ACCELERATING GOAL-CONDITIONED REINFORCEMENT LEARNING ALGORITHMS AND RESEARCH

Anonymous authors
Paper under double-blind review

ABSTRACT

Self-supervision has the potential to transform reinforcement learning (RL), paralleling the breakthroughs it has enabled in other areas of machine learning. While self-supervised learning in other domains aims to find patterns in a fixed dataset, self-supervised goal-conditioneds reinforcement learning (GCRL) agents discover *new* behaviors by learning from the goals achieved during unstructured interaction with the environment. However, these methods have failed to see similar success, both due to a lack of data from slow environment simulations as well as a lack of stable algorithms. We take a step toward addressing both of these issues by releasing a high-performance codebase and benchmark (`JaxGCRL`) for self-supervised GCRL, enabling researchers to train agents for millions of environment steps in minutes on a single GPU. By utilizing GPU-accelerated replay buffers, environments, and a stable contrastive RL algorithm, we reduce training time by up to $22\times$. Additionally, we assess key design choices in contrastive RL, identifying those that most effectively stabilize and enhance training performance. With this approach, we provide a foundation for future research in self-supervised GCRL, enabling researchers to quickly iterate on new ideas and evaluate them in diverse and challenging environments. Code: `https://anonymous.4open.science/r/JaxGCRL-2316/README.md`

1 INTRODUCTION

Self-supervised learning has significantly influenced machine learning over the last decade, transforming how research is done in domains such as natural language processing and computer vision (**?**Dosovitskiy et al., 2020; Vaswani et al., 2017). In the context of reinforcement learning (RL), most self-supervised prior methods apply the same recipe that has been successful in other domains: learning representations or models from a large, fixed dataset (Hoffmann et al., 2022; Sardana et al., 2024; Muennighoff et al., 2023). However, the RL setting also enables a fundamentally different type of self-supervised learning: rather than learning from a fixed dataset (as done in NLP and computer vision), a self-supervised *reinforcement* learner can collect its own dataset. Thus, rather than learning a representation of a dataset, the self-supervised reinforcement learner acquires a representation of an environment or of behaviors and optimal policies therein. Self-supervised reinforcement learners may address many of the challenges that stymie today's foundations models: reasoning about the consequences of actions (Rajani et al., 2019; Kwon et al., 2023) (i.e., counterfactuals (Bhargava and Ng, 2022; Jin et al., 2023)) and long horizon planning (Bhargava and Ng, 2022; Du et al., 2023; Guan et al., 2023).

In this paper, we study self-supervised RL in an online setting: an agent interacts in an environment without a reward to learn representations, which are later used to quickly solve downstream tasks. We focus on goal-conditioned reinforcement learning (GCRL) algorithms, which aim to use these unsupervised interactions to learn policies for achieving various goals – an essential capability for multipurpose robots. Prior work has proposed several algorithms for self-supervised RL (Eysenbach et al., 2022; Zheng et al., 2024; Myers et al., 2023; 2024a), including algorithms that focus on learning goals (Erraqabi et al., 2022). However, these methods were limited by small datasets and infrequent online interactions with the environment, which has prevented them from exploring the potential emergent properties of self-supervised reinforcement learning on large-scale data.

The main goal of this paper is to introduce `JaxGCRL`: extremely *fast* GPU-accelerated codebase and benchmark for effective self-supervised GCRL research. For instance, an experiment with
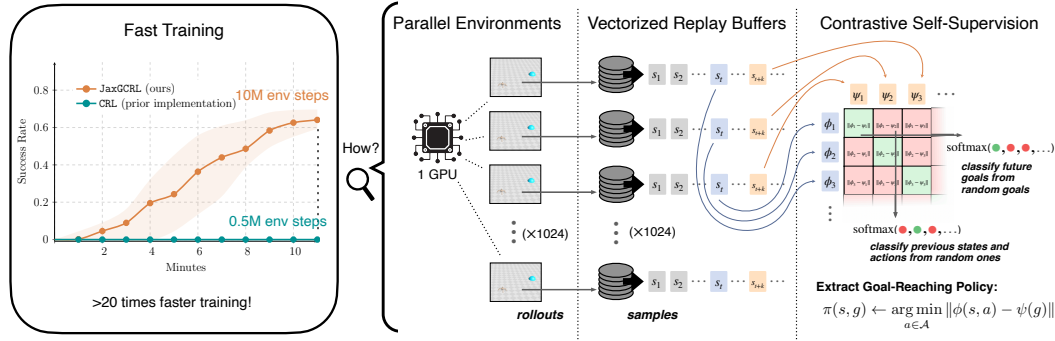
Figure 1: **JaxGCRL is fast.** It learns goal-reaching policies for Ant in 10 minutes on 1 GPU. This paper releases a GCRL benchmark and baseline algorithms that enable research and experiments to be done in minutes.

10 million environment steps lasts only around 10 minutes on a single GPU, which is **up to 22×
faster** than in the original contrastive RL codebase (Eysenbach et al., 2022) (Fig. 1). This speed
allows researchers to "interactively" debug their algorithms, changing pieces and getting results in
near real-time for multiple random seeds on a single GPU without the hustle of distributed training.
Consequently, JaxGCRL eliminates the barriers to entry to state-of-the-art GCRL research, making
it more accessible to under-resourced institutions.

To achieve this training and performance improvement, we combine insights from self-supervised
RL with recent advances in GPU-accelerated simulation. The *first key ingredient* is recent work on
GPU-accelerated simulators, both for physics (Freeman et al., 2021; Thibault et al., 2024; Liang et al.,
2018) and other tasks (Matthews et al., 2024; Dalton et al., 2020; Fischer et al., 2009; Bonnet et al.,
2024; Rutherford et al., 2024) that enable users to collect data up to $1000\times$ faster (Freeman et al.,
2021) than prior methods based on CPUs. The *second key ingredient* is a highly stable algorithm
build upon recent work on contrastive RL (CRL) (Eysenbach et al., 2022; Zheng et al., 2024), which
uses temporal contrastive learning to learn a value function. The *third key ingredient* is a suite of
tasks for evaluating self-supervised RL agents which is not only blazing fast but also stress tests the
exploration and long-horizon reasoning capabilities of RL policies.

The contributions of this work are as follows:

JaxGCRL codebase: a blazingly fast JIT-compiled training pipeline for GCRL experiments.

JaxGCRL benchmark: we introduce a suite of 8 GPU-accelerated state-based environments that
help to accurately assess GCRL algorithm capabilities and limitations.

Extensive empirical analysis: we evaluate important CRL design choices, focusing on key algo-
rithm components, architecture scaling, and training in data-rich settings.

2 RELATED WORK

We build upon recent advances in GCRL, self-supervised RL, and hardware-accelerated physics
simulators, showing that CRL enables fast and reliable training across a diverse suite of environments.

2.1 GOAL-CONDITIONED REINFORCEMENT LEARNING

GCRL is a special case of the general multi-task RL setting, in which the potential tasks are defined
by goal states that the agent is trying to reach in an environment (Kaelbling, 1993; Ghosh et al., 2019;
Nair et al., 2018). Achieving any goal is appealing for generalist agents, as it allows for diverse
behaviors without needing specific reward functions for each task (each state defines a task when
seen as a goal) (Schaul et al., 2015). GCRL techniques have seen success in domains such as robotic
manipulation (Andrychowicz et al., 2017; Eysenbach et al., 2021; Ghosh et al., 2021; Ding et al.,
2022; Walke et al., 2023) and navigation (Shah et al., 2023; Levine and Shah, 2023; Manderson et al.,
2020; Hoang et al., 2021). Recent work has shown that representations of goals can be imbued with
additional structure to enable capabilities such as language grounding (Myers et al., 2023; Ma et al.,
2023), compositionality (Liu et al., 2023; Myers et al., 2024b; Wang et al., 2023), and planning (Park
et al., 2023; Eysenbach et al., 2024). We show how GCRL techniques based on contrastive learning
(Eysenbach et al., 2022) can be scaled with GPU acceleration to enable fast and stable training.

2.2 Accelerating Deep Reinforcement Learning

Deep RL has only recently become practical for many tasks, in part due to improvements in hardware support for these algorithms. Distributed training has enabled RL algorithms to scale across hundreds of GPUs (Mnih et al., 2016; Espeholt et al., 2018; 2020; Hoffman et al., 2022). To resolve the bottleneck of environment interaction with CPU-bound environments, various GPU-accelerated environments have been proposed (Matthews et al., 2024; Freeman et al., 2021; Bonnet et al., 2024; Rutherford et al., 2024; Liang et al., 2018; Dalton et al., 2020; Makoviychuk et al., 2021; Lange, 2022; Lu et al., 2022). Most of these works rely on JAX (Bradbury et al., 2018; Heek et al., 2023; Hennigan et al., 2020), which enables JIT compilation, operator fusion and other components necessary for efficient vectorized code execution. These features significantly accelerate data collection by supporting rollouts in hundreds of parallelized environments. We build on these advances to scale self-supervised RL to data-rich settings.

2.3 Self-Supervised RL

Self-supervised training has enabled key breakthroughs in language modeling and computer vision (Sermanet et al., 2017; Zhu et al., 2020; Devlin et al., 2019; He et al., 2022; Mikolov et al., 2013). In the context of RL, by the term "self-supervised", we mean techniques that can be learned through interaction with an environment without a reward signal. Perhaps the most successful form of self-supervision has been in multi-agent games that can be rapidly simulated, such as Go and Chess, where self-play has enabled the creation of superhuman agents (Silver et al., 2016; 2017; Zha et al., 2021). When learning goal-reaching agents, another basic form of self-supervision is to relabel trajectories as successful demonstrations of the goal that was reached, even if it differs from the original commanded goal (Kaelbling, 1993; Venkattaramanujam et al., 2020). This technique has seen recent adoption as "hindsight experience replay" for various deep RL algorithms (Andrychowicz et al., 2017; Ghosh et al., 2021; Chebotar et al., 2021; Rauber et al., 2021; Eysenbach et al., 2022).

Another perspective on self-supervision is intrinsic motivation, broadly defined as when an agent computes its own reward signal (Barto, 2013). Intrinsic motivation methods include curiosity (Barto, 2013; Bellemare et al., 2016; Baumli et al., 2021), surprise minimization (Berseth et al., 2019; Rhinehart et al., 2021), and empowerment (Klyubin et al., 2005; de Abril and Kanai, 2018; Choi et al., 2021; Myers et al., 2024a). Closely related are skill discovery methods, which aim to construct intrinsic rewards for diverse collections of behavior (Gregor et al., 2016; Eysenbach et al., 2019; Sharma et al., 2020; Kim et al., 2021; Park et al., 2021; Laskin et al., 2022; Park et al., 2024). Self-supervised RL methods have been difficult to scale due to the need for many environment interactions (Franke et al., 2021; Mnih et al., 2015). This work addresses that challenge by offering a fast and scalable contrastive RL algorithm on a benchmark of diverse tasks.

2.4 RL Benchmarks

The RL community has recently started to pay greater attention to how RL research is conducted, reported, and evaluated (Henderson et al., 2018; Jordan et al., 2020; Agarwal et al., 2022). A key issue is a lack of reliable and efficient benchmarks: it becomes hard to rigorously compare novel methods when the number of trials needed to see statistically significant results across diverse settings ranges in the thousands of training hours (Jordan et al., 2024). Some benchmarks that *have* seen adoption include OpenAI gym/Gymnasium (Brockman et al., 2022; Towers et al., 2024), DeepMind Control Suite (Tassa et al., 2018), and D4RL (Fu et al., 2021). More recently, hardware-accelerated versions of some of these benchmarks have been proposed (Gu et al., 2021; Matthews et al., 2024; Koyamada et al., 2023; Makoviychuk et al., 2021; Nikulin et al., 2023). However, the RL community still lacks advanced benchmarks for goal-conditioned methods. We address this gap with `JaxGCRL`, significantly lowering the GCRL evaluation cost and thereby enabling impactful RL research.

3 Preliminaries

In this section, we introduce notation and preliminary definitions for goal-conditioned RL and the contrastive RL method, which serves as the foundation for this work.

In the goal-conditioned reinforcement learning setting, an agent interacts with a controlled Markov process (CMP) $\mathcal{M} = (\mathcal{S}, \mathcal{A}, p, p_0, \gamma)$ to reach arbitrary goals (Kaelbling, 1993; Andrychowicz et al., 2017; Blier et al., 2021). At any time t the agent will observe a state s_t and select a corresponding

action $a_t \in \mathcal{A}$. The dynamics of this interaction are defined by the distribution $p(s_{t+1} \mid s_t, a_t)$, with an initial distribution $p_0(s_0)$ over the state at the start of a trajectory, for $s_t \in \mathcal{S}$ and $a_t \in \mathcal{A}$.

For any goal $g \in \mathcal{S}$, we cast optimal goal-reaching as a problem of inference (Borsa et al., 2019; Barreto et al., 2022; Blier et al., 2021; Eysenbach et al., 2022): given the current state and desired goal, what is the most likely action that will bring us toward that goal? As we will see, this is equivalent to solving the Markov decision process (MDP) $\mathcal{M}_g$ obtained by augmenting $\mathcal{M}$ with the goal-conditioned reward $r_g(s_t, a_t) \triangleq (1 - \gamma)\gamma p(s_{t+1} = g \mid s_t, a_t)$. Formally, a goal-conditioned policy $\pi(a \mid s, g)$ receives both the current observation of the environment as well as a goal $g \in \mathcal{S}$.

We denote the k-step action-conditioned policy distribution $p_k^\pi(s_k \mid s_0, a_0)$ as the distribution of states k steps in the future given the initial state s_0 and action a_0 under π. We define the discounted state visitation distribution as $p_\gamma^\pi(s^+ \mid s, a) \triangleq (1 - \gamma)\sum_{t=0}^{\infty} \gamma^t p_t^\pi(s^+ \mid s, a)$, which we interpret as the distribution of the state T steps in the future for $T \sim \mathrm{Geom}(1 - \gamma)$. This last expression is precisely the Q-function of the policy $\pi(\cdot \mid \cdot, g)$ for the reward r_g: $Q_g^\pi(s, a) \triangleq p_\gamma^\pi(g \mid s, a)$ (see Appendix D.1). For a given distribution over goals $g \sim p_\mathcal{G}$, we can now write the overall objective as

$$\max_{\pi(\cdot|\cdot,\cdot)} \mathbb{E}_{p_0(s_0)p_\mathcal{G}(g)\pi(a_0|s_0,g)}\left[p_\gamma^\pi(g \mid s_0, a_0) \right]. \tag{1}$$

3.1 Contrastive Critic Learning

CRL is an actor-critic method that aims to solve Eq. (1). The critic is represented as a state-action-goal value function $f(s, a, g)$, which provides the likelihood of future states and how various actions influence the likelihood of future states. This function satisfies:

$$f(s, a, g) \propto p_\gamma^\pi(g \mid s, a) = Q_g^\pi(s, a). \tag{2}$$

Therefore, we can treat $f(s, a, g)$ as an approximation of the Q-function and use it to train the actor. This approach builds on previous research that frames learning of this critic as a classification problem (Eysenbach et al., 2022; 2021; Zheng et al., 2023; 2024; Farebrother et al., 2024; Myers et al., 2024b). Training is performed on batches of (s, a, g) to classify whether or not g is the future state corresponding to the trajectory starting from (s, a). Thus, in each sample from batch $(s_i, a_i, g_i) \in \mathcal{B}$ the goal g_i is sampled from the future of the trajectory containing (s_i, a_i).

The family of CRL algorithms consists of the following components: (a) the state-action pair and goal state representations, $\phi(s, a)$ and $\psi(g)$, respectively; (b) the critic, which is defined as an energy function $f_{\phi,\psi}(s, a, g)$, measuring *some* form of similarity between $\phi(s, a)$ and $\psi(g)$; and (c) a contrastive loss function, which is a function of the matrix containing the critic values $\{f_{\phi,\psi}(s_i, a_i, g_j)_{i,j}\}$ over the elements of the batch $\mathcal{B}$. The base contrastive loss we study will be the infoNCE objective (Sohn, 2016), modified to use a symmetrized (Radford et al., 2021) critic parameterized with ℓ_2-distances (Eysenbach et al., 2024). The final objective for the critic can thus be expressed as:

$$\min_{\phi,\psi} \mathbb{E}_\mathcal{B}\left[-\sum_{i=1}^{|\mathcal{B}|} \log\left(\frac{e^{f_{\phi,\psi}(s_i,a_i,g_i)}}{\sum_{j=1}^K e^{f_{\phi,\psi}(s_i,a_i,g_j)}} \right) - \sum_{i=1}^{|\mathcal{B}|} \log\left(\frac{e^{f_{\phi,\psi}(s_i,a_i,g_i)}}{\sum_{j=1}^K e^{f_{\phi,\psi}(s_j,a_j,g_i)}} \right) \right],$$

where

$$f_{\phi,\psi}(s, a, g) = \|\phi(s, a) - \psi(g)\|_2.$$

This loss contrasts each positive sample with the batch of negative samples. Other losses, which are tested in Section 5.3, are further discussed in Appendix A.2.

3.2 Policy Learning

We use a DDPG-style policy extraction loss to learn a goal-conditioned policy, $\pi_\theta(a|s, g)$, by optimizing the critic $f_{\phi,\psi}$ (Lillicrap et al., 2016):

$$\max_\theta \mathbb{E}_{p(s,a)p(g|s,a)\pi_\theta(a'|s,g)}\left[f_{\phi,\psi}(s, a', g) \right] \tag{3}$$

To form a batch of data, we sample uniformly (s, a) pairs and then sample goals g from states that occur after s in a trajectory.
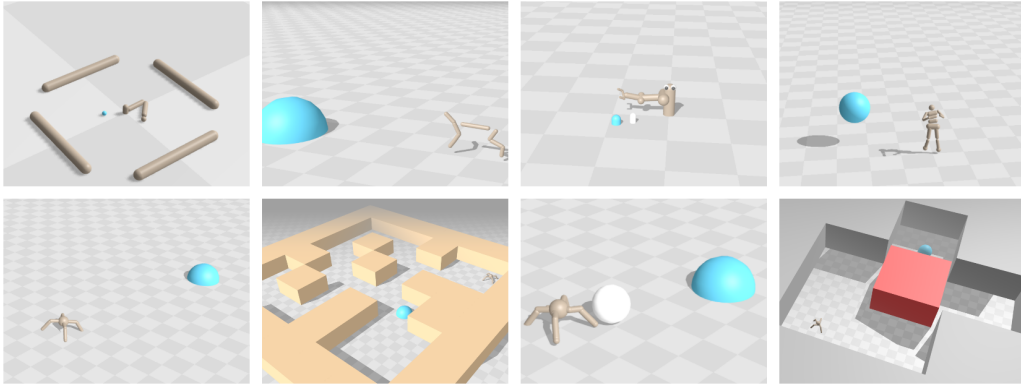
Figure 2: **`JaxGCRL benchmark`**: New suite of GPU-accelerated environments for studying GCRL. In this setting, the agent does not receive any rewards or demonstrations, making some of these tasks an excellent testbed for studying exploration and long-horizon reasoning. Our accompanying implementation of GCRL algorithms trains with more than 15K environment steps per second on a single GPU, enabling rapid experimentation.

4 JAxGCRL: A New Benchmark and Implementation

`JaxGCRL` is an efficient tool for developing and evaluating new GCRL algorithms. It shifts the bottleneck from compute to implementation time, allowing researchers to test new ideas, like contrastive objectives, within minutes—a significant improvement over traditional RL workflows.

4.1 JAxGCRL speedup on a single GPU

We compare the proposed fully JIT-compiled implementation of CRL in `JaxGCRL` to the original implementation from Eysenbach et al. (2022). In particular, Fig. 1 shows the performance in `Ant` environment along with the experiment's wall-clock time. The speedup in this configuration is **22-fold**, with the new implementation reaching a training speed of over 16500 environment steps per second with a 1:16 update to data (UTD) ratio. For results with other UTD, refer to Section 5.6. Complete speedup results are provided in Appendix A.1. Importantly, BRAX physics simulator differs from the original MuJoCo, so performance numbers here may vary slightly from prior work.

4.2 JAxGCRL Environments in the Benchmark

To evaluate the performance of GCRL methods, we propose `JaxGCRL` benchmark consisting of 8 diverse continuous control environments. These environments range from simple, ideal for quick checks, to complex, requiring long-term planning and exploration for success. The following list provides a brief description of each environment, with the technical details summarized in Table 1:

Reacher (Brockman et al., 2022). A 2D manipulation task involves positioning the end part of a 2-segment robotic arm in a specific location sampled uniformly from a disk around an agent.

Half Cheetah (Wawrzyński, 2009). In this 2d task, a 2-legged agent has to get to a goal that is sampled from one of the 2 possible places, one on each side of the starting position.

Pusher (Brockman et al., 2022). This is a 3d robotic task, that consists of a robotic arm and a movable circular object resting on the ground. The goal is to use the arm to push the object into the goal position. With each reset, both position of the goal and movable object are selected randomly.

Ant (Schulman et al., 2016). A re-implementation of the MuJoCo Ant with a quadruped robot that needs to walk to the goal randomly sampled from a circle centred at the starting position.

Ant Maze (Fu et al., 2021). This environment uses the same quadruped model as the previous Ant, but the agent must navigate a maze to reach the target. We prepared 3 different mazes varying in size and difficulty. In each maze, the goals are sampled from a set of listed possible positions.

Ant Soccer (Tunyasuvunakool et al., 2020). In this environment, the Ant has to push a spherical object into a goal position that is sampled uniformly from a circle around the starting position. The position of the movable sphere is randomized on the line between an agent and a goal.

Ant Push (Fu et al., 2021). To reach a goal, the Ant has to push a movable box out of the way. If the box is pushed in the wrong direction, the task becomes unsolvable. Succeeding requires exploration, understanding block dynamics, and how it changes the layout of the maze.

Humanoid (Tassa et al., 2012). Re-implementing the Mujoco task involves navigating a complex humanoid-like robot to walk towards a goal sampled from a disk centred at the starting position.

In Fig. 3, we report the baseline results for the proposed benchmark. It is worth noting that for most environments, experiments involving 50M environment steps can be completed in less than an hour.

4.3 Contrastive RL design choices

`JaxGCRL` streamlines and accelerates the evaluation of new GCRL algorithms, enabling quick assessment of key CRL design choices:

Energy functions. Measuring the similarity between samples can be achieved in various ways, resulting in potentially different agent behaviors. Our analysis in following sections include cosine similarity (Chen et al., 2020), dot product (Radford et al., 2021), and negative L_1 and L_2 distance (Hu et al., 2023), detailed list can be found in Appendix A.2. Even though there is no consensus on the choice of energy functions for temporal representations, recent works showed that they should abide by quasimetric properties (Wang et al., 2023; Myers et al., 2024b).

Contrastive losses. Beside InfoNCE-type losses (van den Oord et al., 2019; Eysenbach et al., 2022), we evaluate FlatNCE-like losses (Chen et al., 2021), and a Monte Carlo version of Forward-Backward unsupervised loss (Touati and Ollivier, 2021). Additionally, we test novel objectives inspired by preference optimization for large language models (Calandriello et al., 2024). Specifically, we evaluate DPO, IPO, and SPPO, which increase the scores of positive samples and reduce the scores of negative ones. A full list of contrastive objectives can be found in Appendix A.2.

Architecture scaling. Scaling neural network architectures to improve performance is a common practice in other areas of deep learning, but it remains relatively underexplored in RL models, as noted in Nauman et al. (2024a;b). Recently, Zheng et al. (2024) showed that CRL might benefit from deeper and wider architectures with Layer Normalization (Ba et al., 2016) for offline CRL in pixel-based environments; we want to examine whether this also holds for online state-based settings.

5 Examples of Fast Experiments Possible with the New Benchmark

The goal of our experiments is twofold: (1) to establish a baseline for the proposed `JaxGCRL` environments, and (2) to evaluate CRL performance in relation to key design choices. In Section 5.1, we define setup that is used for most of the experiments unless explicitly stated otherwise. *First* in Section 5.2, we report baseline results on `JaxGCRL`. *Second*, in Sections 5.3 and 5.4, we try to understand the influence of design choices on CRL learning performance. *Third*, in Section 5.5, we asses those design choices in a data-rich setting with 300M environment steps. *Lastly*, in Section 5.6, we explore the relation between performance and UTD.

5.1 Experimental Setup

Our experiments use `JaxGCRL` suite of simulated environments described in Section 4.2. We evaluate algorithms in an online setting for 50M environment steps. We compare CRL with Soft Actor-Critic (SAC) (Haarnoja et al., 2018), SAC with Hindsight Experience Replay (HER) (Andrychowicz et al., 2017), TD3 (Fujimoto et al., 2018), TD3+HER, and PPO (Schulman et al., 2017). For algorithms with HER, we use *final* strategy relabelling, i.e. relabeling goals with states achieved at the end of the trajectory. In the majority of experiments, we use CRL with L2 energy function, symmetric InfoNCE objective, and a tuneable entropy coefficient for all methods. See Appendix B for details. We use two performance metrics: success rate and time near goal. Success rate measures whether the agent reached the goal at least once during the episode, while time near goal indicates how long the agent stayed close to it. We use a sparse reward for all baselines, with $r = 1$ when the agent is in goal proximity and $r = 0$ otherwise. We define goal-reaching as achieving proximity below the `goal distance` threshold defined in Table 1. The implementations of PPO and SAC are sourced from the Brax repository (Freeman et al., 2021), while TD3, HER, and CRL are partially based on Brax.

5.2 JaxGCRL BENCHMARK RESULTS

We establish baseline results for JaxGCRL with all algorithms in Fig. 3. Clearly, CRL achieves the highest performance across tested methods, resulting in non-trivial policies even in the hardest tasks in terms of high-dimensional state and action spaces (Humanoid) and exploration (Pusher and Ant Push). However, the performance in these challenging environments is low, indicating room for improvement for future contrastive RL methods. As expected, HER can improve performance for both TD3 and SAC. In contrast, PPO performs poorly across all tasks, likely due to the challenges posed by the sparse reward setting. Additional experiments on JaxGCRL environments with design choices discussed in the following sections can be found in Appendix A.4.
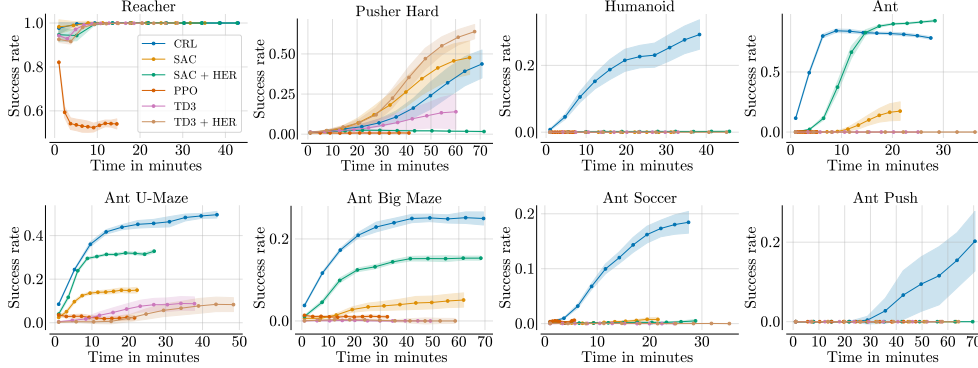

Figure 3: **Baseline results in JaxGCRL benchmark.** Success rates of CRL, SAC, and SAC+HER for 50M environment steps for each JaxGCRL environments. CRL outperforms other baselines in most of the environments. The training speed is a function of the environment complexity, method complexity, and physics backend; see Appendix A.4. Specifically, due to differences in how each methods works, the speed the vary greatly on the same environment, this can be best seen with PPO method being significantly faster than others due to it not using a replay buffer, which frees up GPU memory for more parallel environment simulations. Results are reported as the interquartile mean (IQM) along with its standard error, based on 10 seeds.

5.3 CONTRASTIVE OBJECTIVES AND ENERGY FUNCTIONS COMPARISON

Contrastive objective and energy function are the two main components of contrastive methods, serving as the primary drivers of their final performance. We evaluate CRL with 10 different contrastive objectives, as defined in Section 4.3 across five environments: Ant Soccer, Ant, Ant Big Maze, Ant U-Maze, Ant Push, and Pusher, and report aggregated performance. For the energy function, we use L2, as it consistently resulted in the highest performance for the CRL method, especially regarding time near goal, see Appendix A.2. Additionally, we apply logsumexp regularization with a coefficient of 0.1 to each objective. This auxiliary objective is essential, as without it, the performance of InfoNCE deteriorates significantly (Eysenbach et al., 2022). The analysis presented in Fig. 4 reveals that the originally proposed NCE-binary objective, along with forward-backward, IPO, and SPPO, are the least effective objectives among those evaluated. However, for other InfoNCE-derived objectives, it is difficult to determine the best one, as their performance is similar. Interestingly, CRL seems fairly robust to the choice of contrastive objective.

5.4 SCALING THE ARCHITECTURE

In this section, we explore how increasing the size of actor and critic networks, in terms of both depth and width, influences CRL performance. We evaluate the aggregated performance during the final 10M steps of a 50 million-step training process across three environments: Ant, Ant Soccer, and Ant U-Maze. We use the L2, Symmetric InfoNCE and logsumexp regularizer coefficient of 0.1 for all architecture sizes.

We present the results of this scaling experiment in Fig. 5 and observe that increasing both the width and depth tends to increase performance. However, performance does not further improve when increasing the depth for width = 1024 neurons. Our next experiment studies whether layer
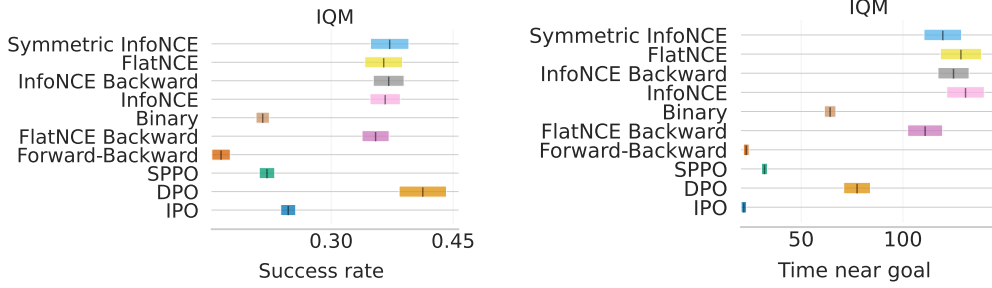
Figure 4: **InfoNCE-based loss functions perform best.** The critic loss functions that achieve the highest success rates are based on InfoNCE and DPO. However, DPO policies tend to stay at the goal for a shorter duration. IQMs averaged over 10 seeds and plotted with one standard error.
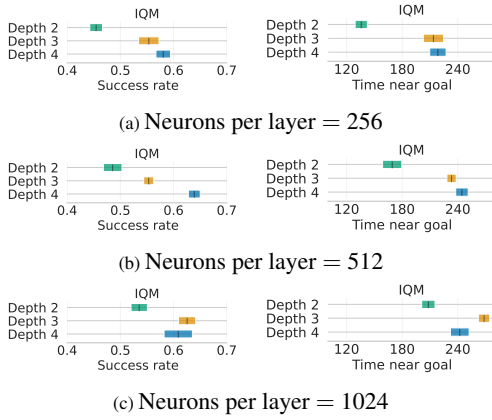

Figure 5: **Scaling the critic and actor networks.** Increasing the width and depth generally enhances performance, but performance levels off for deeper architectures at a width of 1024. Aggregated metrics, 5 seeds per configuration.
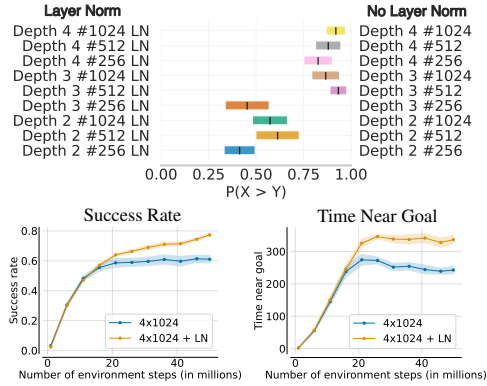
Figure 6: **Layer normalization enables stable performance improvement.** Using Layer Normalization (LN) in the largest architecture allows for continued learning even after reaching the saturation point of a standard large architecture.

normalization can stabilize the performance of these biggest networks (width of 1024 neurons, depth of 4). Indeed, the results in Fig. 6 show that adding layer normalization before every activation allows better scaling properties, especially for bigger networks.

5.5 SCALING THE DATA

We evaluate the benefits CRL gains from training in a data-rich setting. In particular, we report performance for large architectures (studied in Section 5.4) with different combinations of energy functions and contrastive objectives for 300M environment steps in Fig. 7. We observe that the L2 energy function with InfoNCE objective configuration outperforms all others by a substantial margin, leading to a higher success rate and time near the goal across three locomotion tasks. Interestingly, the dot product energy function performs best in the object manipulation task (Ant Soccer). This indicates that only a subset of a wide array of design choices performs well when scaling CRL. Additionally, there is still room for improvement in scaling CRL with data, as the success rate in Ant Soccer and Ant Big Maze remains around 40%. For additional experiments, refer to Appendix A.6

5.6 GRADIENT UPDATES TO DATA RATIO

To achieve a balance between CRL performance and training speed and to examine whether frequent model updates benefit CRL, we evaluate various UTD ratios. In particular, we examine ratios (1:1, 1:8, 1:16, 1:24, 1:32, 1:49, 1:48) in four environments: Ant, Ant Soccer, Ant U-Maze and Pusher Hard. Interestingly, we only observe an increase in performance for Pusher Hard with a higher number of updates, while in other environments, it leads to decreased performance. With a UTD ratio

of 1:16, our code is $22\times$ faster than prior implementations, and with a lower frequency of gradient updates, it can be even faster.
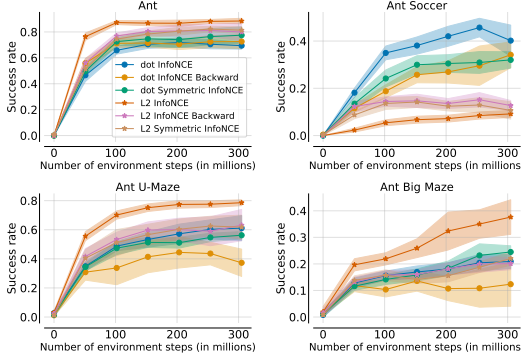

Figure 7: **JaxGCRL allows researchers to study energy functions and critic losses over hundreds of millions of steps.** Among tested configurations, L2 with InfoNCE objective performs best in locomotion environments when data is abundant.
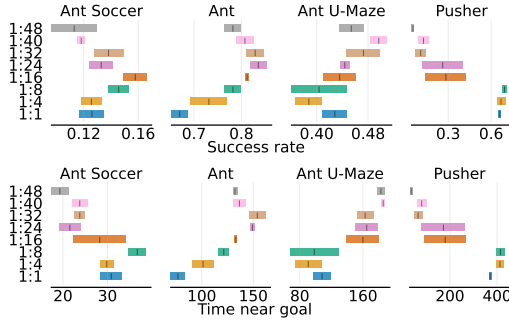
Figure 8: **More gradients $\neq$ better performance.** Success rate (top) and Time near goal (bottom) for different UTD ratios. Increasing the UTD ratio for CRL increases performance only for Pusher.

Key takeaways from empirical experiments:

- **Experiments with 10M steps can be completed in minutes, while those with billions of environment steps can be done in a few hours using JaxGCRL on a single GPU.**

- CRL is the only method that can learn effectively in all proposed environments without needing a high UTD ratio in most cases. It benefits greatly from using large architectures, especially when Layer Normalization is applied.

- Different combinations of energy and contrastive functions lead to different outcomes: some primarily improve success rates, while others extend the time spent near the goal.

Taken together, these experiments not only provide guidance on good design decisions for self-supervised RL, but also highlight how our fast codebase and benchmark can enable researchers to quickly iterate on ideas and hyperparameters.

6 CONCLUSION

In this paper, we introduce JaxGCRL, a very fast benchmark and codebase for goal-conditioned RL. The speed of the new benchmark enables us to rapidly study design choices for state-based CRL, including the network architectures and contrastive losses. We expect that self-supervised RL methods will open the door to entirely new learning algorithms with broad capabilities that go beyond the capabilities of today's foundational models. The key step towards this goal is accelerating and democratising self-supervised RL research so that any lab can carry it out regardless of its computing capabilities. Open-sourcing the proposed codebase with easy-to-implement self-supervised RL methods is an important step in this direction.

Limitations. The GCRL paradigm complicates the process of defining goals that are not easily expressed as a single state, making it infeasible for some applications. Additionally, our benchmark environments and methods assume full observability and that goals are being sampled from known goal distribution during training rollouts. Future work should relax these assumptions to make self-supervised RL agents useful in more practical settings. We also only investigate online GCRL settings.

Reproducibility Statement. All experiments can be replicated using the provided publicly available JaxGCRL code at https://anonymous.4open.science/r/JaxGCRL-2316/README.md. This repository includes comprehensive instructions for setting up the environment, running the experiments, and evaluating the results, making it straightforward to reproduce the findings.

REFERENCES

Rishabh Agarwal, Max Schwarzer, Pablo Samuel Castro, Aaron Courville, and Marc G. Bellemare. Deep Reinforcement Learning at the Edge of the Statistical Precipice. 2022. arXiv:2108.13264.

Marcin Andrychowicz, Filip Wolski, Alex Ray, Jonas Schneider, Rachel Fong, Peter Welinder, Bob McGrew, Josh Tobin, OpenAI Pieter Abbeel, and Wojciech Zaremba. Hindsight Experience Replay. In *Advances in Neural Information Processing Systems*, volume 30. 2017.

Jimmy Lei Ba, Jamie Ryan Kiros, and Geoffrey E. Hinton. Layer Normalization. In *International Conference on Advances in Artificial Intelligence*. 2016.

André Barreto, Will Dabney, Rémi Munos, Jonathan J. Hunt, Tom Schaul, Hado van Hasselt, and David Silver. Successor Features for Transfer in Reinforcement Learning. 2022. Curran Associates, Inc.:arXiv:1606.05312.

Andrew G. Barto. Intrinsic Motivation and Reinforcement Learning. In Gianluca Baldassarre and Marco Mirolli, editors, *Intrinsically Motivated Learning in Natural and Artificial Systems*, pp. 17–47. Springer, 2013.

Kate Baumli, David Warde-Farley, Steven Hansen, and Volodymyr Mnih. Relative Variational Intrinsic Control. In *AAAI Conference on Artificial Intelligence*, volume 35, pp. 6732–6740. 2021.

Marc G. Bellemare, Sriram Srinivasan, Georg Ostrovski, Tom Schaul, David Saxton, and Remi Munos. Unifying Count-Based Exploration and Intrinsic Motivation. In *Conference on Neural Information Processing Systems*. 2016.

Glen Berseth, Daniel Geng, Coline Devin, Nicholas Rhinehart, Chelsea Finn, Dinesh Jayaraman, and Sergey Levine. Smirl: Surprise Minimizing Reinforcement Learning in Unstable Environments. In *International Conference on Learning Representations*. 2019.

Prajjwal Bhargava and Vincent Ng. Commonsense Knowledge Reasoning and Generation With Pre-Trained Language Models: A Survey. 2022.

Léonard Blier, Corentin Tallec, and Yann Ollivier. Learning Successor States and Goal-Dependent Values: A Mathematical Viewpoint. 2021. arXiv:2101.07123.

Clément Bonnet, Daniel Luo, Donal Byrne, Shikha Surana, Sasha Abramowitz, Paul Duckworth, Vincent Coyette, Laurence I. Midgley, et al. Jumanji: A Diverse Suite of Scalable Reinforcement Learning Environments in JAX. In *International Conference on Learning Representations*. 2024.

Diana Borsa, André Barreto, John Quan, Daniel Mankowitz, Rémi Munos, Hado van Hasselt, David Silver, and Tom Schaul. Universal Successor Features Approximators. In *International Conference on Learning Representations*. 2019.

James Bradbury, Roy Frostig, Peter Hawkins, Matthew James Johnson, Chris Leary, Dougal Maclaurin, George Necula, Adam Paszke, Jake VanderPlas, Skye Wanderman-Milne, and Qiao Zhang. JAX: Composable Transformations of Python+Numpy Programs. 2018.

Greg Brockman, Vicki Cheung, Ludwig Pettersson, Jonas Schneider, John Schulman, Jie Tang, and Wojciech Zaremba. Openai Gym. In *J. Open Source Softw*. 2022.

Daniele Calandriello, Daniel Guo, Remi Munos, Mark Rowland, Yunhao Tang, Bernardo Avila Pires, Pierre Harvey Richemond, Charline Le Lan, et al. Human Alignment of Large Language Models Through Online Preference Optimisation. 2024. arXiv:2403.08635.

Yevgen Chebotar, Karol Hausman, Yao Lu, Ted Xiao, Dmitry Kalashnikov, Jake Varley, Alex Irpan, Benjamin Eysenbach, Ryan Julian, Chelsea Finn, et al. Actionable Models: Unsupervised Offline Reinforcement Learning of Robotic Skills. In *International Conference on Machine Learning*. 2021.

Junya Chen, Zhe Gan, Xuan Li, Qing Guo, Liqun Chen, Shuyang Gao, Tagyoung Chung, Yi Xu, et al. Simpler, Faster, Stronger: Breaking the Log-K Curse on Contrastive Learners With Flatnce. 2021. arXiv:2107.01152.

Ting Chen, Simon Kornblith, Mohammad Norouzi, and Geoffrey Hinton. A Simple Framework for Contrastive Learning of Visual Representations. 2020. arXiv:2002.05709.

Jongwook Choi, Archit Sharma, Honglak Lee, Sergey Levine, and Shixiang Shane Gu. Variational Empowerment as Representation Learning for Goal-Conditioned Reinforcement Learning. In *International Conference on Machine Learning*, pp. 1953–1963. 2021.

Steven Dalton, Iuri Frosio, and Michael Garland. Accelerating Reinforcement Learning Through GPU Atari Emulation. In *Conference on Neural Information Processing Systems*. 2020.

Ildefons Magrans de Abril and Ryota Kanai. A Unified Strategy for Implementing Curiosity and Empowerment Driven Reinforcement Learning. 2018. arXiv:1806.06505.

Jacob Devlin, Ming-Wei Chang, Kenton Lee, and Kristina Toutanova. BERT: Pre-Training of Deep Bidirectional Transformers for Language Understanding. In *Annual Conference of the North American Chapter of the Association for Computational Linguistics*. 2019.

Wenhao Ding, Haohong Lin, Bo Li, and Ding Zhao. Generalizing Goal-Conditioned Reinforcement Learning With Variational Causal Reasoning. In *Conference on Neural Information Processing Systems*. 2022.

A. Dosovitskiy, L. Beyer, Alexander Kolesnikov, Dirk Weissenborn, Xiaohua Zhai, Thomas Unterthiner, M. Dehghani, Matthias Minderer, G. Heigold, S. Gelly, Jakob Uszkoreit, and N. Houlsby. an Image Is Worth 16x16 Words: Transformers for Image Recognition at Scale. *International Conference on Learning Representations*, 2020.

Yuqing Du, Eliza Kosoy, Alyssa Dayan, Maria Rufova, Pieter Abbeel, and Alison Gopnik. What Can AI Learn From Human Exploration? Intrinsically-Motivated Humans and Agents in Open-World Exploration. In *Neurips 2023 Workshop: Information-Theoretic Principles in Cognitive Systems*. 2023.

Akram Erraqabi, Marlos C. Machado, Mingde Zhao, Sainbayar Sukhbaatar, Alessandro Lazaric, Ludovic Denoyer, and Yoshua Bengio. Temporal Abstractions-Augmented Temporally Contrastive Learning: an Alternative to the Laplacian in RL. 2022. arXiv:2203.11369.

Lasse Espeholt, Raphaël Marinier, Piotr Stanczyk, Ke Wang, and Marcin Michalski. SEED RL: Scalable and Efficient Deep-RL With Accelerated Central Inference. In *International Conference on Learning Representations*. 2020.

Lasse Espeholt, Hubert Soyer, Remi Munos, Karen Simonyan, Volodymir Mnih, Tom Ward, Yotam Doron, Vlad Firoiu, Tim Harley, Iain Dunning, Shane Legg, and Koray Kavukcuoglu. IMPALA: Scalable Distributed Deep-Rl With Importance Weighted Actor-Learner Architectures. In *International Conference on Machine Learning*. 2018.

Benjamin Eysenbach, Abhishek Gupta, Julian Ibarz, and Sergey Levine. Diversity Is All You Need: Learning Skills Without a Reward Function. In *International Conference on Learning Representations*. 2019.

Benjamin Eysenbach, Vivek Myers, Ruslan Salakhutdinov, and Sergey Levine. Inference via Interpolation: Contrastive Representations Provably Enable Planning and Inference. In *Conference on Neural Information Processing Systems*. 2024.

Benjamin Eysenbach, Ruslan Salakhutdinov, and Sergey Levine. C-Learning: Learning to Achieve Goals via Recursive Classification. In *International Conference on Learning Representations*. 2021.

Benjamin Eysenbach, Tianjun Zhang, Sergey Levine, and Russ R. Salakhutdinov. Contrastive Learning as Goal-Conditioned Reinforcement Learning. In *Advances in Neural Information Processing Systems*, volume 35, pp. 35603–35620. 2022.

Jesse Farebrother, Jordi Orbay, Quan Vuong, Adrien Ali Taiga, Yevgen Chebotar, Ted Xiao, Alex Irpan, Sergey Levine, Pablo Samuel Castro, and Aleksandra Faust. Stop Regressing: Training Value Functions via Classification for Scalable Deep RL. In *Forty-First International Conference on Machine Learning*, arXiv:2403.03950. 2024.

Leonardo G. Fischer, Renato Silveira, and Luciana Nedel. Gpu Accelerated Path-Planning for Multi-Agents in Virtual Environments. In *2009 VIII Brazilian Symposium on Games and Digital Entertainment*, pp. 101–110. 2009.

Jörg K. H. Franke, Gregor Köhler, André Biedenkapp, and Frank Hutter. Sample-Efficient Automated Deep Reinforcement Learning. In *International Conference on Learning Representations*. 2021.

C. Daniel Freeman, Erik Frey, Anton Raichuk, Sertan Girgin, Igor Mordatch, and Olivier Bachem. Brax – a Differentiable Physics Engine for Large Scale Rigid Body Simulation. In *Neurips Datasets and Benchmarks*. 2021.

Justin Fu, Aviral Kumar, Ofir Nachum, George Tucker, and Sergey Levine. D4RL: Datasets for Deep Data-Driven Reinforcement Learning. 2021. arXiv:2004.07219.

Scott Fujimoto, Herke van Hoof, and David Meger. Addressing Function Approximation Error in Actor-Critic Methods. In Jennifer G. Dy and Andreas Krause, editors, *Proceedings of the 35th International Conference on Machine Learning, ICML 2018, Stockholmsmässan, Stockholm,*

Sweden, July 10-15, 2018, volume 80 of *Proceedings of Machine Learning Research*, pp. 1582–1591. 2018.

Dibya Ghosh, Abhishek Gupta, and Sergey Levine. Learning Actionable Representations With Goal-Conditioned Policies. In *International Conference on Learning Representations*. 2019.

Dibya Ghosh, Abhishek Gupta, Ashwin Reddy, Justin Fu, Coline Devin, Benjamin Eysenbach, and Sergey Levine. Learning to Reach Goals via Iterated Supervised Learning. In *International Conference on Learning Representations*. 2021.

Karol Gregor, Danilo Jimenez Rezende, and Daan Wierstra. Variational Intrinsic Control. *International Conference on Learning Representations*, 2016.

Shixiang Shane Gu, Manfred Diaz, Daniel C. Freeman, Hiroki Furuta, Seyed Kamyar Seyed Ghasemipour, Anton Raichuk, Byron David, Erik Frey, Erwin Coumans, and Olivier Bachem. Braxlines: Fast and Interactive Toolkit for Rl-Driven Behavior Engineering Beyond Reward Maximization. 2021. arXiv:2110.04686.

Lin Guan, Karthik Valmeekam, Sarath Sreedharan, and Subbarao Kambhampati. Leveraging Pre-Trained Large Language Models to Construct and Utilize World Models for Model-Based Task Planning. In *Advances in Neural Information Processing Systems*, volume 36, pp. 79081–79094. 2023.

Tuomas Haarnoja, Aurick Zhou, P. Abbeel, and S. Levine. Soft Actor-Critic: Off-Policy Maximum Entropy Deep Reinforcement Learning With a Stochastic Actor. *International Conference on Machine Learning*, 2018.

Kaiming He, Xinlei Chen, Saining Xie, Yanghao Li, Piotr Dollár, and Ross Girshick. Masked Autoencoders Are Scalable Vision Learners. In *IEEE/CVF Conference on Computer Vision and Pattern Recognition*. 2022.

Jonathan Heek, Anselm Levskaya, Avital Oliver, Marvin Ritter, Bertrand Rondepierre, Andreas Steiner, and Marc van Zee. Flax: A Neural Network Library and Ecosystem for JAX. 2023.

Peter Henderson, Riashat Islam, Philip Bachman, Joelle Pineau, Doina Precup, and David Meger. Deep Reinforcement Learning That Matters. In *AAAI Conference on Artificial Intelligence*. 2018.

Tom Hennigan, Trevor Cai, Tamara Norman, Lena Martens, and Igor Babuschkin. Haiku: Sonnet for JAX. 2020.

Christopher Hoang, Sungryull Sohn, Jongwook Choi, Wilka Carvalho, and Honglak Lee. Successor Feature Landmarks for Long-Horizon Goal-Conditioned Reinforcement Learning. In *Advances in Neural Information Processing Systems*, volume 34, pp. 26963–26975. 2021.

Matthew W. Hoffman, Bobak Shahriari, John Aslanides, Gabriel Barth-Maron, Nikola Momchev, Danila Sinopalnikov, Piotr Stańczyk, Sabela Ramos, et al. Acme: A Research Framework for Distributed Reinforcement Learning. 2022. arXiv:2006.00979.

Jordan Hoffmann, Sebastian Borgeaud, Arthur Mensch, Elena Buchatskaya, Trevor Cai, Eliza Rutherford, Diego de Las Casas, Lisa Anne Hendricks, et al. Training Compute-Optimal Large Language Models. 2022. arXiv:2203.15556.

Tianyang Hu, Zhili Liu, Fengwei Zhou, Wenjia Wang, and Weiran Huang. Your Contrastive Learning Is Secretly Doing Stochastic Neighbor Embedding. In *International Conference on Learning Representations*. 2023.

Zhijing Jin, Yuen Chen, Felix Leeb, Luigi Gresele, Ojasv Kamal, L. Y. U. Zhiheng, Kevin Blin, Fernando Gonzalez Adauto, Max Kleiman-Weiner, and Mrinmaya Sachan. Cladder: Assessing Causal Reasoning in Language Models. In *Thirty-Seventh Conference on Neural Information Processing Systems*. 2023.

Scott Jordan, Yash Chandak, Daniel Cohen, Mengxue Zhang, and Philip Thomas. Evaluating the Performance of Reinforcement Learning Algorithms. In *International Conference on Machine Learning*, pp. 4962–4973. 2020.

Scott M. Jordan, Adam White, Bruno Castro da Silva, Martha White, and Philip S. Thomas. Position: Benchmarking Is Limited in Reinforcement Learning Research. 2024. arXiv:2406.16241.

Leslie Pack Kaelbling. Learning to Achieve Goals. In *International Joint Conference on Artificial Intelligence*. 1993.

Jaekyeom Kim, Seohong Park, and Gunhee Kim. Unsupervised Skill Discovery With Bottleneck Option Learning. In *International Conference on Machine Learning*. 2021.

Alexander S Klyubin, Daniel Polani, and Chrystopher L Nehaniv. Empowerment: A Universal Agent-Centric Measure of Control. In *2005 IEEE Congress on Evolutionary Computation*, volume 1, pp. 128–135. 2005.

Sotetsu Koyamada, Shinri Okano, Soichiro Nishimori, Yu Murata, Keigo Habara, Haruka Kita, and Shin Ishii. Pgx: Hardware-Accelerated Parallel Game Simulators for Reinforcement Learning. *Advances in Neural Information Processing Systems*, 36:45716–45743, 2023.

Minae Kwon, Hengyuan Hu, Vivek Myers, Siddharth Karamcheti, A. Dragan, and Dorsa Sadigh. Toward Grounded Commonsense Reasoning. In *International Conference on Robotics and Automation*. 2023.

Robert Tjarko Lange. gymnax: A JAX-based Reinforcement Learning Environment Library. 2022.

Michael Laskin, Hao Liu, Xue Bin Peng, Denis Yarats, Aravind Rajeswaran, and Pieter Abbeel. CIC: Contrastive Intrinsic Control for Unsupervised Skill Discovery. 2022. arXiv:2202.00161.

Sergey Levine and Dhruv Shah. Learning Robotic Navigation From Experience: Principles, Methods, and Recent Results. *Philosophical Transactions of the Royal Society B: Biological Sciences*, 378(1869):20210447, 2023.

Jacky Liang, Viktor Makoviychuk, Ankur Handa, Nuttapong Chentanez, Miles Macklin, and Dieter Fox. Gpu-Accelerated Robotic Simulation for Distributed Reinforcement Learning. In *Proceedings of the 2nd Conference on Robot Learning*, pp. 270–282. 2018.

Timothy P. Lillicrap, Jonathan J. Hunt, Alexander Pritzel, Nicolas Heess, Tom Erez, Yuval Tassa, David Silver, and Daan Wierstra. Continuous Control With Deep Reinforcement Learning. In *International Conference on Learning Representations*. 2016.

Bo Liu, Yihao Feng, Qiang Liu, and Peter Stone. Metric Residual Network for Sample Efficient Goal-Conditioned Reinforcement Learning. In *AAAI Conference on Artificial Intelligence*, volume 37, pp. 8799–8806. 2023.

Chris Lu, Jakub Kuba, Alistair Letcher, Luke Metz, Christian Schroeder de Witt, and Jakob Foerster. Discovered policy optimisation. *Advances in Neural Information Processing Systems*, 35:16455–16468, 2022.

Yecheng Jason Ma, William Liang, Vaidehi Som, Vikash Kumar, Amy Zhang, Osbert Bastani, and Dinesh Jayaraman. LIV: Language-Image Representations and Rewards for Robotic Control. In *International Conference on Machine Learning*. 2023.

Viktor Makoviychuk, Lukasz Wawrzyniak, Yunrong Guo, Michelle Lu, Kier Storey, Miles Macklin, David Hoeller, Nikita Rudin, Arthur Allshire, Ankur Handa, and Gavriel State. Isaac Gym: High Performance GPU-Based Physics Simulation for Robot Learning. In *Neurips Datasets and Benchmarks*. 2021.

Travis Manderson, Juan Camilo Gamboa Higuera, Stefan Wapnick, Jean-François Tremblay, Florian Shkurti, David Meger, and Gregory Dudek. Vision-Based Goal-Conditioned Policies for Underwater Navigation in the Presence of Obstacles. In *Robotics - Science and Systems*. 2020.

Michael Matthews, Michael Beukman, Benjamin Ellis, Mikayel Samvelyan, Matthew Thomas Jackson, Samuel Coward, and Jakob Nicolaus Foerster. Craftax: A Lightning-Fast Benchmark for Open-Ended Reinforcement Learning. In *Forty-First International Conference on Machine Learning*. 2024.

Tomas Mikolov, Ilya Sutskever, Kai Chen, Greg S Corrado, and Jeff Dean. Distributed Representations of Words and Phrases and Their Compositionality. In *Advances in Neural Information Processing Systems*, volume 26. 2013.

Volodymyr Mnih, Adrià Puigdomènech Badia, Mehdi Mirza, Alex Graves, Timothy P. Lillicrap, Tim Harley, David Silver, and Koray Kavukcuoglu. Asynchronous Methods for Deep Reinforcement Learning. In *International Conference on Machine Learning*. 2016.

Volodymyr Mnih, Koray Kavukcuoglu, David Silver, Andrei A. Rusu, Joel Veness, Marc G. Bellemare, Alex Graves, Martin Riedmiller, et al. Human-Level Control Through Deep Reinforcement Learning. *Nature*, 518(7540):529–533, 2015.

Niklas Muennighoff, Alexander Rush, Boaz Barak, Teven Le Scao, Nouamane Tazi, Aleksandra Piktus, Sampo Pyysalo, Thomas Wolf, and Colin A. Raffel. Scaling Data-Constrained Language Models. In *Advances in Neural Information Processing Systems*, volume 36, pp. 50358–50376. 2023.

Vivek Myers, Evan Ellis, Sergey Levine, Benjamin Eysenbach, and Anca Dragan. Learning to Assist Humans Without Inferring Rewards. In *Conference on Neural Information Processing Systems*. 2024a.

Vivek Myers, Andre Wang He, Kuan Fang, Homer Rich Walke, Philippe Hansen-Estruch, Ching-An Cheng, Mihai Jalobeanu, Andrey Kolobov, Anca Dragan, and Sergey Levine. Goal Representations for Instruction Following: A Semi-Supervised Language Interface to Control. In *Conference on Robot Learning*, pp. 3894–3908. 2023.

Vivek Myers, Chongyi Zheng, Anca Dragan, Sergey Levine, and Benjamin Eysenbach. Learning Temporal Distances: Contrastive Successor Features Can Provide a Metric Structure for Decision-Making. In *International Conference on Machine Learning*, arXiv:2406.17098. 2024b.

Ashvin V Nair, Vitchyr Pong, Murtaza Dalal, Shikhar Bahl, Steven Lin, and Sergey Levine. Visual Reinforcement Learning With Imagined Goals. In *Advances in Neural Information Processing Systems*, volume 31. 2018.

Michal Nauman, Michał Bortkiewicz, Piotr Miłoś, Tomasz Trzcinski, Mateusz Ostaszewski, and Marek Cygan. Overestimation, Overfitting, and Plasticity in Actor-Critic: the Bitter Lesson of Reinforcement Learning. In *Forty-First International Conference on Machine Learning*, arXiv:2403.00514. 2024a.

Michal Nauman, Mateusz Ostaszewski, Krzysztof Jankowski, Piotr Miłoś, and Marek Cygan. Bigger, Regularized, Optimistic: Scaling for Compute and Sample-Efficient Continuous Control. 2024b.

Alexander Nikulin, Vladislav Kurenkov, Ilya Zisman, Artem Agarkov, Viacheslav Sinii, and Sergey Kolesnikov. Xland-Minigrid: Scalable Meta-Reinforcement Learning Environments in JAX. 2023.

Seohong Park, Jongwook Choi, Jaekyeom Kim, Honglak Lee, and Gunhee Kim. Lipschitz-Constrained Unsupervised Skill Discovery. In *International Conference on Learning Representations*. 2021.

Seohong Park, Dibya Ghosh, Benjamin Eysenbach, and Sergey Levine. HIQL: Offline Goal-Conditioned RL With Latent States as Actions. In *Conference on Neural Information Processing Systems*. 2023.

Seohong Park, Oleh Rybkin, and Sergey Levine. METRA: Scalable Unsupervised RL With Metric-Aware Abstraction. In *International Conference on Learning Representations*. 2024.

Alec Radford, Jong Wook Kim, Chris Hallacy, Aditya Ramesh, Gabriel Goh, Sandhini Agarwal, Girish Sastry, Amanda Askell, Pamela Mishkin, Jack Clark, Gretchen Krueger, and Ilya Sutskever. Learning Transferable Visual Models From Natural Language Supervision. In *International Conference on Machine Learning*, arXiv:2103.00020. 2021.

Nazneen Fatema Rajani, Bryan McCann, Caiming Xiong, and Richard Socher. Explain Yourself! Leveraging Language Models for Commonsense Reasoning. In *Association for Computational Linguistics*, pp. 4932–4942. 2019.

Paulo Rauber, Avinash Ummadisingu, Filipe Mutz, and Juergen Schmidhuber. Hindsight Policy Gradients. In *Neural Comput.* 2021.

Nicholas Rhinehart, Jenny Wang, Glen Berseth, John Co-Reyes, Danijar Hafner, Chelsea Finn, and Sergey Levine. Information Is Power: Intrinsic Control via Information Capture. In *Advances in Neural Information Processing Systems*, volume 34, pp. 10745–10758. 2021.

Alexander Rutherford, Benjamin Ellis, Matteo Gallici, Jonathan Cook, Andrei Lupu, Garðar Ingvarsson, Timon Willi, Akbir Khan, Christian Schroeder de Witt, and Alexandra Souly. Jaxmarl: Multi-Agent RL Environments in JAX. In *Second Agent Learning in Open-Endedness Workshop*. 2024.

Nikhil Sardana, Jacob Portes, Sasha Doubov, and Jonathan Frankle. Beyond Chinchilla-Optimal: Accounting for Inference in Language Model Scaling Laws. In *International Conference on Machine Learning*. 2024.

Tom Schaul, Dan Horgan, Karol Gregor, and David Silver. Universal Value Function Approximators. In *32nd International Conference on Machine Learning*, pp. 1312–1320. 2015.

John Schulman, Philipp Moritz, Sergey Levine, Michael Jordan, and Pieter Abbeel. High-Dimensional Continuous Control Using Generalized Advantage Estimation. In *International Conference on Learning Representations*. 2016.

John Schulman, Filip Wolski, Prafulla Dhariwal, Alec Radford, and Oleg Klimov. Proximal Policy Optimization Algorithms. *arXiv preprint arXiv: 1707.06347*, 2017.

Pierre Sermanet, Corey Lynch, Jasmine Hsu, and Sergey Levine. Time-Contrastive Networks: Self-Supervised Learning From Multi-View Observation. In *2017 IEEE Conference on Computer Vision and Pattern Recognition Workshops*, pp. 486–487. 2017.

Dhruv Shah, Ajay Sridhar, Nitish Dashora, Kyle Stachowicz, Kevin Black, Noriaki Hirose, and Sergey Levine. Vint: A Foundation Model for Visual Navigation. In *Conference on Robot Learning*. 2023.

Archit Sharma, Shixiang Gu, Sergey Levine, Vikash Kumar, and Karol Hausman. Dynamics-Aware Unsupervised Discovery of Skills. In *International Conference on Learning Representations*. 2020.

David Silver, Aja Huang, Chris J. Maddison, Arthur Guez, Laurent Sifre, George van den Driessche, Julian Schrittwieser, Ioannis Antonoglou, et al. Mastering the Game of Go With Deep Neural Networks and Tree Search. *Nature*, 529(7587):484–489, 2016.

David Silver, Thomas Hubert, Julian Schrittwieser, Ioannis Antonoglou, Matthew Lai, Arthur Guez, Marc Lanctot, Laurent Sifre, et al. Mastering Chess and Shogi by Self-Play With a General Reinforcement Learning Algorithm. 2017. arXiv:1712.01815.

Kihyuk Sohn. Improved Deep Metric Learning With Multi-Class N-Pair Loss Objective. In *Advances in Neural Information Processing Systems*, volume 29. 2016.

Yuval Tassa, Yotam Doron, Alistair Muldal, Tom Erez, Yazhe Li, Diego de Las Casas, David Budden, Abbas Abdolmaleki, Josh Merel, Andrew Lefrancq, Timothy Lillicrap, and Martin Riedmiller. Deepmind Control Suite. 2018. arXiv:1801.00690.

Yuval Tassa, Tom Erez, and Emanuel Todorov. Synthesis and Stabilization of Complex Behaviors Through Online Trajectory Optimization. In *2012 IEEE/RSJ International Conference on Intelligent Robots and Systems*, pp. 4906–4913. 2012.

William Thibault, William Melek, and Katja Mombaur. Learning Velocity-Based Humanoid Locomotion: Massively Parallel Learning With Brax and MJX. 2024. arXiv:2407.05148.

Emanuel Todorov, Tom Erez, and Yuval Tassa. Mujoco: A Physics Engine for Model-Based Control. In *2012 IEEE/RSJ International Conference on Intelligent Robots and Systems*, pp. 5026–5033. 2012.

Ahmed Touati and Yann Ollivier. Learning One Representation to Optimize All Rewards. In *Conference on Neural Information Processing Systems*, volume 34, pp. 13–23. 2021.

Mark Towers, Ariel Kwiatkowski, Jordan Terry, John U. Balis, Gianluca De Cola, Tristan Deleu, Manuel Goulão, Andreas Kallinteris, et al. Gymnasium: A Standard Interface for Reinforcement Learning Environments. 2024. arXiv:2407.17032.

Saran Tunyasuvunakool, Alistair Muldal, Yotam Doron, Siqi Liu, Steven Bohez, Josh Merel, Tom Erez, Timothy Lillicrap, Nicolas Heess, and Yuval Tassa. Dm_control: Software and Tasks for Continuous Control. *Software Impacts*, 6:100022, 2020.

Aaron van den Oord, Yazhe Li, and Oriol Vinyals. Representation Learning With Contrastive Predictive Coding. 2019. arXiv:1807.03748.

Ashish Vaswani, Noam M. Shazeer, Niki Parmar, Jakob Uszkoreit, Llion Jones, Aidan N. Gomez, Lukasz Kaiser, and Illia Polosukhin. Attention Is All You Need. *Conference on Neural Information Processing Systems*, 2017.

Srinivas Venkattaramanujam, Eric Crawford, Thang Doan, and Doina Precup. Self-Supervised Learning of Distance Functions for Goal-Conditioned Reinforcement Learning. 2020. arXiv:1907.02998.

Homer Rich Walke, Kevin Black, Tony Z. Zhao, Quan Vuong, Chongyi Zheng, Philippe Hansen-Estruch, Andre Wang He, Vivek Myers, et al. Bridgedata V2: A Dataset for Robot Learning at Scale. In *Conference on Robot Learning*, pp. 1723–1736. 2023.

Tongzhou Wang, Antonio Torralba, Phillip Isola, and Amy Zhang. Optimal Goal-Reaching Reinforcement Learning via Quasimetric Learning. In *International Conference on Machine Learning*. 2023.

Paweł Wawrzyński. A Cat-Like Robot Real-Time Learning to Run. In Mikko Kolehmainen, Pekka Toivanen, and Bartlomiej Beliczynski, editors, *Adaptive and Natural Computing Algorithms*, pp. 380–390. 2009.

Daochen Zha, Jingru Xie, Wenye Ma, Sheng Zhang, Xiangru Lian, Xia Hu, and Ji Liu. Douzero: Mastering Doudizhu With Self-Play Deep Reinforcement Learning. In *International Conference on Machine Learning*, pp. 12333–12344. 2021.

Chongyi Zheng, Benjamin Eysenbach, Homer Walke, Patrick Yin, Kuan Fang, Ruslan Salakhutdinov, and Sergey Levine. Stabilizing Contrastive RL: Techniques for Offline Goal Reaching. In *International Conference on Learning Representations*. 2024.

Chongyi Zheng, Ruslan Salakhutdinov, and Benjamin Eysenbach. Contrastive Difference Predictive Coding. In *the Twelfth International Conference on Learning Representations*. 2023.

Yizhe Zhu, Martin Renqiang Min, Asim Kadav, and Hans Peter Graf. S3vae: Self-Supervised Sequential Vae for Representation Disentanglement and Data Generation. In *IEEE/CVF Conference on Computer Vision and Pattern Recognition*, pp. 6538–6547. 2020.

A   ADDITIONAL RESULTS

A.1   SPEEDUP COMPARISON ACROSS VARIOUS NUMBERS OF PARALLEL ENVIRONMENTS

We present an extended version of the plot from Fig. 1, with additional experiments, as depicted on the left side of Fig. 9. Each experiment was run for 10M environment steps, and for the original repository, we varied the number of parallel actors for data collection, testing configurations with 4, 8, 16, and 32 actors, each running on separate CPU threads. Each configuration was tested with three different random seeds, and we present the results along with the corresponding standard deviations. The novel repository used 1024 actors for data collection. We used NVIDIA V100 GPU for this experiment.

A notable observation from these experiments is the variation in success rates associated with different numbers of parallel actors. We hypothesize that this discrepancy arises due to the increased diversity of data supplied to the replay buffer as the number of independent parallel environments increases, leading to more varied experiences for each policy update. We conducted similar experiments using our method with varying numbers of parallel environments to further investigate. The results are presented on the right side of Fig. 9. This observation, while interesting, is beyond the scope of the current work and is proposed as an area for further investigation.
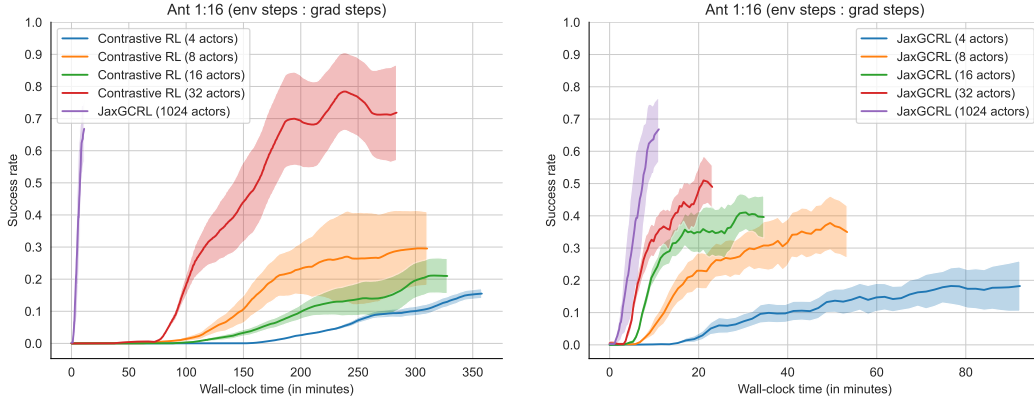

Figure 9: Speedup in ant environment for the 1:16 ratio of SGD steps : environment steps for different numbers of parallel actors.

A.2   ENERGY FUNCTIONS AND CONTRASTIVE OBJECTIVES

The full list of evaluated energy functions:

$$f_{\phi,\psi,\cos}(s,a,g) = \frac{\langle \phi(s,a), \psi(g) \rangle}{\|\phi(s,a)\|_2 \|\psi(g)\|_2}, \tag{4}$$

$$f_{\phi,\psi,\mathrm{dot}}(s,a,g) = \langle \phi(s,a), \psi(g) \rangle, \tag{5}$$

$$f_{\phi,\psi,L_1}(s,a,g) = -\|\phi(s,a) - \psi(g)\|_1, \tag{6}$$

$$f_{\phi,\psi,L_2}(s,a,g) = -\|\phi(s,a) - \psi(g)\|_2, \tag{7}$$

$$f_{\phi,\psi,L_{2\ w\backslash o\ sqrt}}(s,a,g) = -\|\phi(s,a) - \psi(g)\|_2^2. \tag{8}$$
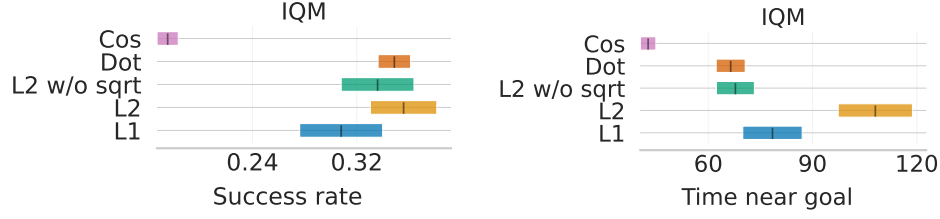
16

Figure 10: **Energy functions influence CRL performance metrics in multiple ways.** Success rate (left) and time near goal (right) results for 5 energy functions. IQMs indicate better performance of p-norms and dot product as energy functions over cosine similarity for CRL. Interestingly, L2 results in a much higher time near goal than other energy functions. Results averaged over five seeds and plotted with one standard error.

The full list of tested contrastive objectives:

$$\mathcal{L}_{\text{InfoNCE-fwd}}(\mathcal{B}; \phi, \psi) = -\sum_{i=1}^{|\mathcal{B}|} \log\left(\frac{e^{f_{\phi,\psi}(s_i, a_i, \textcolor{green}{g_i})}}{\sum_{j=1}^{K} e^{f_{\phi,\psi}(s_i, a_i, \textcolor{red}{g_j})}}\right), \tag{9}$$

$$\mathcal{L}_{\text{InfoNCE-bwd}}(\mathcal{B}; \phi, \psi) = -\sum_{i=1}^{|\mathcal{B}|} \log\left(\frac{e^{f_{\phi,\psi}(s_i, a_i, \textcolor{green}{g_i})}}{\sum_{j=1}^{K} e^{f_{\phi,\psi}(\textcolor{red}{s_j, a_j}, g_i)}}\right), \tag{10}$$

$$\mathcal{L}_{\text{InfoNCE-sym}}(\mathcal{B}; \phi, \psi) = \mathcal{L}_{\text{InfoNCE-fwd}}(\mathcal{B}; \phi, \psi) + \mathcal{L}_{\text{InfoNCE-bwd}}(\mathcal{B}; \phi, \psi), \tag{11}$$

$$\mathcal{L}_{\text{FlatNCE-fwd}}(\mathcal{B}; \phi, \psi) = -\sum_{i=1}^{|\mathcal{B}|} \log\left(\frac{\sum_{j=1}^{|\mathcal{B}|} e^{f_{\phi,\psi}(s_i, a_i, \textcolor{red}{g_j}) - f_{\phi,\psi}(s_i, a_i, \textcolor{green}{g_i})}}{\texttt{detach}\left[\sum_{j=1}^{|\mathcal{B}|} e^{f_{\phi,\psi}(s_i, a_i, \textcolor{red}{g_j}) - f_{\phi,\psi}(s_i, a_i, \textcolor{green}{g_i})}\right]}\right), \tag{12}$$

$$\mathcal{L}_{\text{FlatNCE-bwd}}(\mathcal{B}; \phi, \psi) = -\sum_{i=1}^{|\mathcal{B}|} \log\left(\frac{\sum_{j=1}^{|\mathcal{B}|} e^{f_{\phi,\psi}(\textcolor{red}{s_j, a_j}, g_i) - f_{\phi,\psi}(s_i, a_i, \textcolor{green}{g_i})}}{\texttt{detach}\left[\sum_{j=1}^{|\mathcal{B}|} e^{f_{\phi,\psi}(\textcolor{red}{s_j, a_j}, g_i) - f_{\phi,\psi}(s_i, a_i, \textcolor{green}{g_i})}\right]}\right), \tag{13}$$

$$\mathcal{L}_{\text{FB}}(\mathcal{B}; \phi, \psi) = -\sum_{i=1}^{|\mathcal{B}|} \left(e^{f_{\phi,\psi}(s_i, a_i, \textcolor{green}{g_i})}\right) + \frac{1}{2(|\mathcal{B}|-1)} \sum_{j=1, j\neq i}^{K} \left(e^{f_{\phi,\psi}(s_i, a_i, \textcolor{red}{g_j})}\right)^2, \tag{14}$$

$$\mathcal{L}_{\text{DPO}}(\mathcal{B}; \phi, \psi) = -\sum_{i=1}^{|\mathcal{B}|} \sum_{j=1}^{|\mathcal{B}|} \log \sigma\left[f_{\phi,\psi}(s_i, a_i, \textcolor{green}{g_i}) - f_{\phi,\psi}(s_i, a_i, \textcolor{red}{g_j})\right], \tag{15}$$

$$\mathcal{L}_{\text{IPO}}(\mathcal{B}; \phi, \psi) = \sum_{i=1}^{|\mathcal{B}|} \sum_{j=1}^{|\mathcal{B}|} \left[\left(f_{\phi,\psi}(s_i, a_i, \textcolor{green}{g_i}) - f_{\phi,\psi}(s_i, a_i, \textcolor{red}{g_j})\right) - 1\right]^2, \tag{16}$$

$$\mathcal{L}_{\text{SPPO}}(\mathcal{B}; \phi, \psi) = \sum_{i=1}^{|\mathcal{B}|} \sum_{j=1}^{|\mathcal{B}|} \left[f_{\phi,\psi}(s_i, a_i, \textcolor{green}{g_i}) - 1\right]^2 + \left[f_{\phi,\psi}(s_i, a_i, \textcolor{red}{g_j}) + 1\right]^2, \tag{17}$$

where we have highlighted the indices corresponding to positive and negative samples for clarity.

The last three of those losses, that is DPO, IPO, and SPPO were *inspired* by the structure of losses in the Preference Optimization domain. Unlike in the losses from InfoNCE family, here the samples are compared in pairs.
The DPO loss simply drives the difference between scores of positive and negative samples to be larger, and doesn't regularize those scores in any other way.
The IPO loss can be seen as a restriction of DPO, where the scores are regularized to always have a difference of one between a positive and negative sample pairs.
The SPPO loss restricts this even further, and regularizes the scores to be equal to one for positive samples and negative one for negative samples.

A.3 ENERGY FUNCTIONS RESULTS

The performance of contrastive learning is sensitive to energy function choice (Sohn, 2016). This section aims to understand how different energy functions impact CRL performance. In particular, we evaluate five energy functions: L1, L2, L2 w/o sqrt, dot product and cosine. For every energy function, we use symmetric InfoNCE as a contrastive objective, with a 0.1 logsumexp penalty coefficient.

In Fig. 10, we report the performance of every energy function for four different ant environments and pusher. We find that p-norms and dot-product significantly outperform cosine similarity. Additionally,

removing the root square from the L2 norm (L2 w/o sqrt) results in performance degradation, especially regarding time near goal. This modification makes the energy function no longer abide by the triangle inequality, which, as pointed out by (Myers et al., 2024b), is desirable for temporal contrastive features. Results per environment are reported in Fig. 11.

Fig. 11 shows the results of different energy functions per environment, success rate and time near goal. Clearly, no single energy function performs well in all the tested environments, as, for instance, L1 and L2, which perform well in Ant environments, work poorly in Pusher. In addition, we observed high variability in every configuration performance, as indicated by relatively wide standard errors.
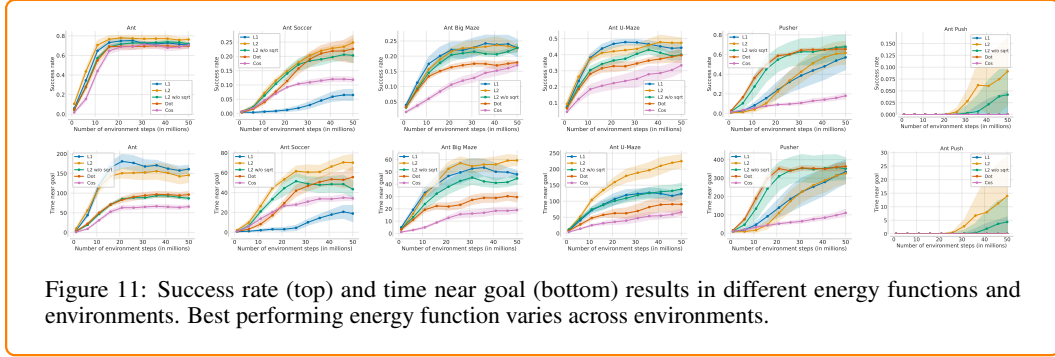

Figure 11: Success rate (top) and time near goal (bottom) results in different energy functions and environments. Best performing energy function varies across environments.

A.4 BENCHMARK PERFORMANCE

In this section, report additional results for more advanced architectures on the benchmark environment. In particular, we report the results for architecture with 4 hidden layers of size 1024 and Layer Normalization in Fig. 12. Unsurprisingly, the performance is significantly better in most environments, particularly for Humanoid. This suggests that a larger architecture is needed to effectively manage the high-dimensional state and action spaces involved in this environment.
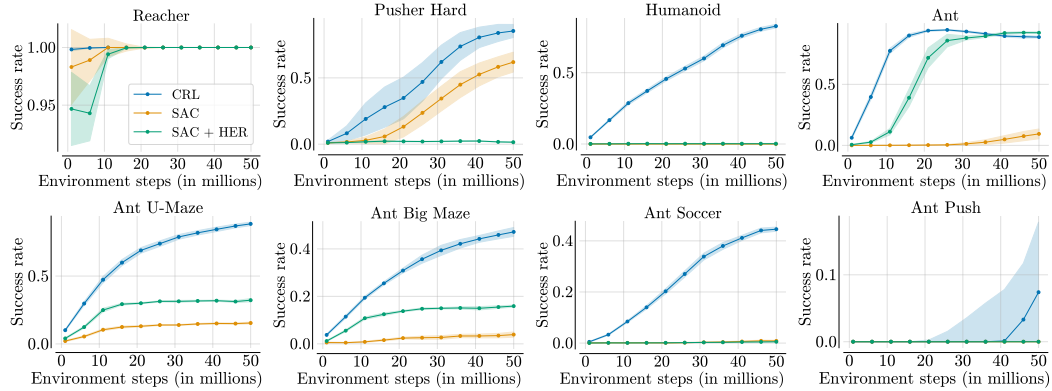

Figure 12: **Baseline results in JaxGCRL benchmark.** Success rates for each of our benchmark environments using bigger architecture. Reported as 10 seeds and standard error.

A.5 HINDSIGHT EXPERIENCE REPLAY DETAILS

In HER, we relabel, on average, 50% of goals with states achieved at the end of the rollout. The humanoid environment was trained on goals sampled from a distance in the range $[1.0, 5.0]$ meters and evaluated on goals sampled from a distance 5.0 meters. All other environments were trained and evaluated on identical environments.

We observe poor performance for SAC+HER in the Pusher environment as a result of HER generating a "successful" experience, which is trivial. In particular, the goal in the pusher environment is the desired location of the puck, which is different from its initial position, so that agent should *push* the puck to that position. Relabeling the goal to the final location of the puck reached at the end of the

episode often results in just changing the goal to the puck's initial position. This happens because, during the early stages of training, the random policy usually doesn't interact with the puck.

A.6 SCALED-UP CRL ARCHITECTURE IN DATA-RICH SETTING

In Figures 13 and 14, we report success rates and time near goal for scaled-up CRL agent with architecture consisting of 4 layers with 1024 neurons per layer and layer norm. We find that these architectures can increase the fraction of trials where the agent reaches the goal at least once, but they do not enable the agent to stabilise around the goal (e.g., on 5 tasks, the best agent spends less than 50% of an episode at the goal). When visualizing the rollouts, we observe that the Humanoid agent falls immediately after reaching the goal state, and the Ant Soccer agent struggles to recover when it pushes the ball too far away.
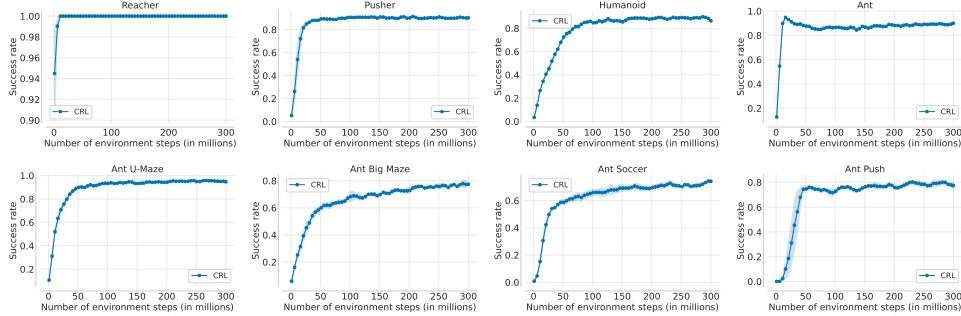

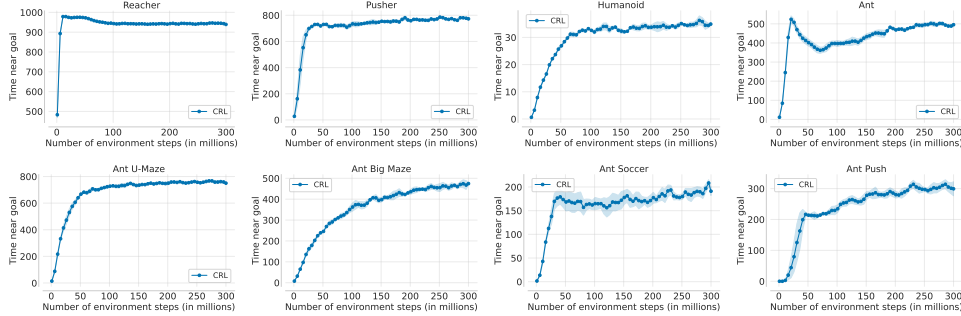Figure 13: **CRL with big architecture success rates in data-rich setting.**

Figure 14: **CRL with big architecture time near goal in data-rich setting.**

B TECHNICAL DETAILS

`JaxGCRL` is a fast implementation of state-based self-supervised reinforcement learning algorithms and a new benchmark of GPU-accelerated environments. Our implementation leverages the power of GPU-accelerated simulators (BRAX and MuJoCo MJX) (Freeman et al., 2021; Todorov et al., 2012) to reduce the time required for data collection and training, allowing researchers to run extensive experiments in a fraction of the time previously needed. The bottleneck of former self-supervised RL implementations was twofold. Firstly, data collection was executed on many CPU threads, as a single thread was often used for a single actor. This reduced the number of possible parallel workers, as only high-compute servers could run hundreds of parallel actors. Secondly, the necessity of data migration between CPU (data collection) and GPU (training) posed additional overhead. These two problems are mitigated by fully JIT-compiled algorithm implementation and execution of all environments and replay buffer operations directly on the GPU.

Notably, our implementation uses only one CPU thread and has low RAM usage as all the operations, including those on the replay buffer, are computed on GPU. It's important to note that the BRAX physics simulator is not exactly the same as the original MuJoCo simulator, so the performance numbers reported here are slightly different from those in prior work. All methods and baselines we report are run on the same BRAX simulator.

B.1 ENVIRONMENT DETAILS

In each of the environments, there are a number of parameters that can change the learning process. A non-exhaustive list of such details for each environment is presented below.

Table 1: Environments details

Environment	Goal distance	Termination	Brax pipeline	Goal sampling
Reacher	0.05	No	Spring	Disc with radius sampled from $[0.0, 0.2]$
Half-Cheetah	0.5	No	MJX	Fixed goal location
Pusher Easy	0.1	No	Generalized	x coordinate sampled from $[-0.55, -0.25]$, y coordinate sampled from $[-0.2, 0.2]$
Pusher Hard	0.1	No	Generalized	x coordinate sampled from $[-0.65, 0.35]$, y coordinate sampled from $[-0.55, 0.45]$
Humanoid	0.5^1	Yes	Spring	Disc with radius sampled from $[1.0, 5.0]$
Ant	0.5	Yes	Spring	Circle with radius 10.0
Ant Maze	0.5	Yes	Spring	Maze specific
Ant Soccer	0.5	Yes	Spring	Circle with radius 5.0
Ant Push	0.5	Yes	MJX	Two possible locations with uniform noise added

B.2 BENCHMARK DETAILS

Our experiments use `JaxGCRL` suite of simulated environments described in Section 4.2. We evaluate algorithms in an online setting, with a UTD ratio 1:16 for CRL, TD3, TD3+HER, SAC, SAC+HER, and $1:5$ for PPO. We use a batch size of 256 and a discount factor of 0.99 for all methods except PPO, for which we use a discount factor of 0.97. For every environment, we sample evaluation goals from the same distribution as training ones and use a replay buffer of size 10M for CRL, TD3, TD3+HER, SAC, and SAC+HER. We use 1024 parallel environments for all methods except for PPO, where we use 4096 parallel environments to collect data. All experiments are conducted for 50 million environment steps.

B.3 BENCHMARK PARAMETERS

The parameters used for benchmarking experiments can be found in Table 2.
`min_replay_size` is a parameter that controls how many transitions **per environment** should be gathered to prefill the replay buffer.
`max_replay_size` is a parameter that controls how many transitions are maximally stored in replay buffer **per environment**.

C RANDOM GOALS

Our loss in Eq. (3) differs from the original CRL algorithm (Eysenbach et al., 2022) by sampling goals from the same trajectories as states during policy extraction, rather than random goals from the replay buffer. Mathematically, we can generalize Eq. (3) to account for either of these strategies by adding a hyperparameter α to the loss controlling the degree of random goal sampling during training.

---

[1]in 3 dimensions

Table 2: Hyperparameters

Hyperparameter	Value
num_timesteps	50,000,000
max_replay_size	10,000
min_replay_size	1,000
episode_length	1,000
discounting	0.99
num_envs	1024 (512 for humanoid)
batch_size	256
multiplier_num_sgd_steps	1
action_repeat	1
unroll_length	62
policy_lr	6e-4
critic_lr	3e-4
contrastive_loss_function	symmetric_infonce
energy_function	L2
logsumexp_penalty	0.1
hidden layers (for both encoders and actor)	[256,256]
representation dimension	64

$$\max_{\theta} \quad (1 - \alpha) \cdot \mathbb{E}_{p(s,a)p(g|s,a)\pi_\theta(a'|s,g)} \left[f_{\phi,\psi}(s, a', g) \right]$$

$$+ \alpha \cdot \mathbb{E}_{p(s,a)p(g)\pi_\theta(a'|s,g)} \left[f_{\phi,\psi}(s, a', g) \right]$$

The hyperparameter α controls the rate of counterfactual goal learning, where the policy is updated based on the critic's evaluation of goals that did not actually occur in the trajectory. We find that taking, $\alpha = 0$ (i.e., no random goal sampling) leads to better performance, and suggest using the policy loss in Eq. (3) for training contrastive RL methods.

D PROOFS

D.1 Q-FUNCTION IS PROBABILITY

This proof follows closely the one presented in Eysenbach et al. (2022).

We want to relate the Q-function to discounted state visitation distribution: $Q_g^\pi(s, a) = p_\gamma^\pi(g \mid s, a)$. The Q-function is usually defined in terms of rewards:

$$Q_g^\pi(s, a) \triangleq \mathbb{E}_{\pi(\cdot|g)} \left[\sum_{t=0}^{\infty} \gamma^t r_g(s_t, a_t) \mid {}^{s_0=s,}_{a_0=a} \right]. \tag{18}$$

We will define rewards conditioned with goal g as:

$$r_g(s, a) \triangleq \begin{cases} (1 - \gamma)\big(p(s_0 = g) + \gamma p(s_1 = g \mid s_0, a_0)\big), & t = 0 \\ (1 - \gamma)\gamma p(s_{t+1} = g \mid s_t, a_t), & t > 0. \end{cases} \tag{19}$$

Lastly, we define discounted state visitation distribution:

$$p_\gamma^\pi(g) \triangleq (1 - \gamma) \sum_{t=0}^{\infty} \gamma^t p_t^\pi(g). \tag{20}$$

For $t > 0$, the term $p_t^\pi(g)$ is a probability of reaching the goal g at timestep t with policy conditioned on g, and thus:

$$p_t^\pi(g) = \mathbb{E}_{\pi(\cdot|g)} \big[p_t(g \mid s_{t-1}, a_{t-1}) \big]$$
$$= \mathbb{E}_{\pi(\cdot|g)} \big[p(s_t = g \mid s_{t-1}, a_{t-1}) \big].$$

On the second line, we have used the Markov property. We can now substitute this into Eq. (20):

$$p_\gamma^\pi(g) = (1 - \gamma) \sum_{t=0}^\infty \gamma^t p_t^\pi(g)$$

$$= (1 - \gamma)p_0^\pi(g) + (1 - \gamma) \sum_{t=1}^\infty \gamma^t \mathbb{E}_{\pi(\cdot|g)}\left[p(s_t = g \mid s_{t-1}, a_{t-1})\right]$$

$$= (1 - \gamma)p_0^\pi(g) + (1 - \gamma) \sum_{t=0}^\infty \gamma^{t+1} \mathbb{E}_{\pi(\cdot|g)}\left[p(s_{t+1} = g \mid s_t, a_t)\right]$$

$$= \mathbb{E}_{\pi(\cdot|g)}\left[(1 - \gamma)p(s_0 = g) + (1 - \gamma) \sum_{t=0}^\infty \gamma^{t+1} p(s_{t+1} = g \mid s_t, a_t)\right]$$

$$= \mathbb{E}_{\pi(\cdot|g)}\left[\underbrace{(1 - \gamma)\left(p(s_0 = g) + \gamma p(s_1 = g \mid s_0, a_0)\right)}_{r_g(s_0, a_0)} + \sum_{t=1}^\infty \gamma^t \underbrace{(1 - \gamma)\gamma p(s_{t+1} = g \mid s_t, a_t)}_{r_g(s_t, a_t)}\right]$$

$$= \mathbb{E}_{\pi(\cdot|g)}\left[\sum_{t=0}^\infty \gamma^t r_g(s_t, a_t)\right].$$

Thus for a set state-action pair (s, a), we have:

$$p_\gamma^\pi(g \mid s, a) = \mathbb{E}_{\pi(\cdot|g)}\left[\sum_{t=0}^\infty \gamma^t r_g(s_t, a_t) \mid {}_{a_0=a}^{s_0=s,}\right] = Q_g^\pi(s, a),$$

which relates the Q-function to discounted state visitation distribution.

E FAILED EXPERIMENTS

1. *Weight Decay:* Prior work (Nauman et al., 2024b) indicated that regularizing critic weights might improve learning stability. We did not observe significant upgrades in the CRL setup, perhaps due to a much lower ratio of updates per environment step. We tested this only for small architectures.

2. *Random Goals:* In prior implementation (Eysenbach et al., 2022) using random goals in actor loss resulted in higher performance. We did not observe that in our online setting.

F PSEUDOCODE

Algorithm 1 Contrastive Reinforcement Learning

1: **Input:** Contrastive loss $\mathcal{L}_{\text{Critic}}$, energy function f
2: Initialize ϕ, ψ, π and an empty replay buffer $\mathcal{D}$
3: **repeat**
4:     **In parallel for each environment instance:**
5:         Observe state s and sample an action $a \sim \pi(s, g)$
6:         Execute a in the environment
7:         Observe next state s' and done signal d to indicate whether s' is terminal
8:         Append (s, a, s') to current trajectory for this environment
9:         **if** s' is terminal **then**
10:           Reset this environment state (this includes sampling new goal)
11:           Store current trajectory for this environment in $\mathcal{D}$
12:           Start new trajectory for this environment
13:     **if** it is time to update **then**
14:         **for** j in range(number of updates) **do**
15:           From buffer $\mathcal{D}$ randomly sample (with discount) a batch $\mathcal{B}$ of state-action pairs and goals from their future
16:           Update critic by one step of gradient descent using given Critic loss:

$$\nabla_{\phi, \psi}\, \mathcal{L}_{\text{Critic}}(\mathcal{B}; \phi, \psi) + \beta \mathcal{L}_{\text{logsumexp}}(\mathcal{B}, \phi, \psi)$$

17:           Update policy by one step of gradient descent using:

$$\nabla_{\pi}\, \mathcal{L}_{\text{Actor}}(\mathcal{B}; \phi, \psi, \pi)$$

18: **until** convergence